ORIGINAL ARTICLE

Therapeutic Effects of Combination of Nebivolol and Donepezil: Targeting Multifactorial Mechanisms in ALS

Soo Yeon Lee[1] · Hye-Yeon Cho[1] · Jung-Pyo Oh[1] · Jiae Park[1] · Sang-Hun Bae[1] · Haesun Park[1] · Eun Jung Kim[1] ·
Ji-Hyun Lee[1]

Abstract

Amyotrophic lateral sclerosis (ALS) is a fatal neurodegenerative disorder characterized by progressive loss of motor neurons in the spinal cord. Although the disease's pathophysiological mechanism remains poorly understood, multifactorial mechanisms affecting motor neuron loss converge to worsen the disease. Although two FDA-approved drugs, riluzole and edaravone, targeting excitotoxicity and oxidative stress, respectively, are available, their efficacies are limited to extending survival by only a few months. Here, we developed combinatorial drugs targeting multifactorial mechanisms underlying key components in ALS disease progression. Using data analysis based on the genetic information of patients with ALS-derived cells and pharmacogenomic data of the drugs, a combination of nebivolol and donepezil (nebivolol-donepezil) was identified for ALS therapy. Here, nebivolol-donepezil markedly reduced the levels of cytokines in the microglial cell line, inhibited nuclear factor-κB (NF-κB) nucleus translocation in the HeLa cell and substantially protected against excitotoxicity-induced neuronal loss by regulating the PI3K-Akt pathway. Nebivolol-donepezil significantly promoted the differentiation of neural progenitor cells (NPC) into motor neurons. Furthermore, we verified the low dose efficacy of nebivolol-donepezil on multiple indices corresponding to the quality of life of patients with ALS in vivo using SOD1^{G93A} mice. Nebivolol-donepezil delayed motor function deterioration and halted motor neuronal loss in the spinal cord. Drug administration effectively suppressed muscle atrophy by mitigating the proportion of smaller myofibers and substantially reducing phospho-neurofilament heavy chain (pNF-H) levels in the serum, a promising ALS biomarker. High-dose nebivolol-donepezil significantly prolonged survival and delayed disease onset compared with vehicle-treated mice. These results indicate that the combination of nebivolol-donepezil efficiently prevents ALS disease progression, benefiting the patients' quality of life and life expectancy.

Keywords Amyotrophic lateral sclerosis · Neurodegeneration · Neuromuscular disease · Drug therapy · SOD1

Introduction

Amyotrophic lateral sclerosis (ALS) is a lethal neuromuscular disease that progressively deteriorates motor neurons in the spinal cord and brain with severe muscle atrophy.

Soo Yeon Lee and Hye-Yeon Cho contributed equally to this work and are co-first authors.

✉ Eun Jung Kim
  ejkim@drnoahbiotech.com

✉ Ji-Hyun Lee
  jhlee@drnoahbiotech.com

1 DR. NOAH BIOTECH Inc., 91, Changnyong-daero
   256beon-gil, Yeongtong-gu, Suwon-si, Gyeonggi-do 16229,
   Republic of Korea

Degeneration begins in the limb and bulbar muscles and spreads across the body, eventually leading to muscle weakness, wasting, respiratory failure, and death within 3–5 years of the first diagnosis [1]. Although the number of patients has dramatically increased, the currently available FDA approved drugs, riluzole and edaravone, could extend survival by a few months with meager functional improvement [2–6].

The pathophysiology of ALS involves multiple complex processes and pathways at the tissue, cellular, and molecular levels. This makes drug development particularly challenging, and ALS remains incurable despite vigorous efforts to combat the disease. At the tissue level, ALS pathophysiology involves inflammatory responses activated by reactive astrocytes and microglia [7–9] and overproduction of inflammatory cytokines [10, 11]. Neuroinflammation is observed even in the earliest stages of ALS, emphasizing

its role in the development and progression of the disease. At the motor neuron level, deficits occur in the neuromuscular junction (NMJ) [12, 13], axons [14, 15], mitochondria [16–18], and/or the cell nucleus [19]. Finally, at the molecular level, several players are suspected of causing the disease, including glutamate excitotoxicity [20, 21] and reactive oxygen species [22].

Multiple clinical studies have suggested that therapeutic approaches targeting multifactorial mechanisms using combined drugs can successfully treat CNS disorders caused by various pathophysiologies. For example, a recent clinical trial of combinatorial therapy for multitargeting disease pathology has been registered at ClinicalTrials.gov (NCT04019704). The trial showed a significant antidepressant effect in patients with major depressive disorder, providing a novel mechanism of action and reducing the side effects of current antidepressants. In addition, a phase III clinical trial of a combinatorial drug, sodium phenylbutyrate-taurursodiol, which reduced neuronal death by mitigating endoplasmic reticulum stress and mitochondrial dysfunction in patients with ALS, was successful in slowing functional decline.

Accordingly, the approach of drug development targeting multifactorial mechanisms using combinatorial drugs is essential to attenuate ALS disease progression compared with the trials that have been developed so far.

Here, we discovered a novel combinatorial drug for ALS therapy that reverses multiple pathological dysfunctions, including motor neuronal loss. We used our proprietary artificial intelligence (AI)-based screening technology that can predict the candidates of combinatorial drugs based on the genomes of patients with ALS and pharmacogenomics, along with an in vitro screening system to evaluate the drug's therapeutic effect. To slow down the progression of ALS using drug combinations targeting multiple mechanisms, a combination of nebivolol-hydrochloride (HCl) and donepezil-HCl (nebivolol-donepezil), FDA-approved drugs originally approved for lowering blood pressure and dementia, respectively, were finally selected.

After screening experiments, we further validated the therapeutic effect of nebivolol-donepezil in multiple systems. In vitro, nebivolol-donepezil significantly reduced inflammatory cytokines induced by lipopolysaccharide (LPS) stimulation and effectively protected against excitotoxicity-induced neuronal loss. In addition, nebivolol-donepezil considerably promoted neurogenesis, enhancing the differentiation of motor neurons from NPC. Subsequently, we verified the therapeutic effect of oral administration of nebivolol-donepezil to SOD1^{G93A} transgenic (TG) mice under the two-dose regimens. Low-dose nebivolol-donepezil administration before motor deterioration significantly improved functional degeneration with reduced muscle atrophy compared with vehicle-treated SOD1^{G93A} TG mice. Moreover, treatment with a high-dose drug combination after symptom onset until death substantially prolonged survival.

Based on these results, we propose nebivolol-donepezil as a potential therapeutic drug for ALS treatment to prevent disease progression in patients with ALS.

Materials and Methods

Data Analysis

To process the expression data, we collected seven (six for microarray and one for RNA-seq) ALS datasets, which were from motor neurons and induced pluripotent stem cells in the gene expression omnibus (GEO) database (Table S1) [23–30]. WGCNA [31] or pathological networks, including subnetworks, were generated using the seven transcriptomic datasets. To measure the connectivity between pathological networks and small molecules, we used pharmacogenomic data from drugs that had passed phase II in clinical trials and extracted the small molecule-induced expression data from the LINCS L1000 project [32]. Furthermore, to identify gene expression signatures representing ALS, the most upregulated and downregulated genes were extracted from each network constructed using WGCNA and defined as a set of ALS signature genes believed to be most relevant to the disease. Finally, we compared the ranks (ranked by log fold change) of signature genes that were identified from the gene expression analysis in each pathological network with those (ranked by Z-score) of the genes in chemical-induced expression data with a rank-based non-parametric test [33], resulting in CS at the modular level. To predict drugs in the context of ALS therapeutic targets, more emphasis was placed on the extent of co-regulation of genes relevant to anti-inflammatory and cell differentiation, which was reflected in calculating the final CS. To discover combinatorial drugs, synergy was predicted by calculating CS and rank aggregation scores, which were based on the non-parametric Kolmogorov–Smirnov test. However, the two methods were applied differently according to the analysis purpose. The schematic workflow for the entire process and algorithms used in our analysis is depicted in Fig. S1.

Animals and Drugs

All animal experiments were conducted according to the MFDS guidelines for the maintenance and use of animals and were approved by IACUC (IACUC number: KBIO-IACUC-2022–090 and KNOTUS IACUC 20-KE-405). Male TG mice ($n = 57$) for human SOD1 G93A (B6SJL.SOD1-G93A) and their male wild-type (WT) littermates ($n = 10$) were used in the experiments. Male SOD1^{G93A} and female B6SJL WT mice were purchased from Jackson Laboratories

and bred to produce F1 mice. Mouse ear or tail samples were collected at the age of 15–21 days for genotype confirmation through PCR analysis. PCR was conducted using forward and reverse primers for the SOD1 transgene (5'-CATCAG CCCTAATCCATCTGA-3'; 5'-CGCGACTAACAATCA AAGTGA-3') and the positive control gene (5'-CTAGGC CACAGAATTGAAAGATCT-3'; 5'-GTAGGTGGAAAT TCTAGCATCA TCC-3'). The heterozygous offspring were selected for experiments. We used only the male mice for consistency and stability of results, as discrepancy is found in disease onset, behavior performance, muscle strength, etc. between male and female SOD1 mutants. TG male mice were designated to Veh or drug-treated groups such that the average weights among the groups were comparable. Nebivolol-HCl (nebivolol), donepezil-HCl (donepezil), or a mixture of nebivolol and donepezil (referred to as nebivolol-donepezil) was administered once daily via oral gavage. Notably, the animals in the vehicle group were administered saline in the same manner. In addition, nebivolol (Cat. CS-2142, Cat.S1549) was purchased from AbaChemScene and Selleckchem for in vivo and in vitro experiments, respectively, and donepezil (Cat. B1602) was purchased from ApexBio.

NO Assay and MTT Assay

BV2 microglial cells were plated in 96-well plates at 2×10^5 cells per well in DMEM high glucose medium (Welgene, LM001-05) supplemented with 10% fetal bovine serum (FBS; YOUNG IN, US-FBS-500) and 1% penicillin–streptomycin (P-S; Gibco, 15070063). Six hours after cell seeding, BV2 microglial cells were treated with the drugs and 1 µg/ml LPS (Sigma, L4391) and incubated (37 °C/5% CO$_2$) for 18 h. After incubation, NO levels were quantified from half of the cell media using a Griess reagent assay kit (Promega, G2930). The assay was performed

following the manufacturer's instructions. Colorimetric changes in the media and Griess reagent mixture were measured using a Synergy HTX Multi-Mode reader (Biotek) at 540 nm. The remaining half of the BV2 cell media was treated with 5 µg/ml of MTT (Thiazolyl Blue Tetrazolium Bromide, Sigma, M5655) solution at 37 °C for 1 h, and 100 µl MTT solvent (DMSO) was added to each well. Colorimetric changes in the solvent were measured using a Synergy HTX Multi-Mode reader (Biotek) at 590 nm.

Quantitative Real-Time PCR (qRT-PCR)

Total RNA was extracted using Easy-Blue reagent (iNtRON Biotechnology, #17,061). Reverse transcription was performed using an iScript cDNA synthesis kit (Bio-Rad, #108,890). Furthermore, qRT-PCR reactions were performed in triplicate using iQ SYBR Green Supermix (Bio-Rad, #170–8880) on a CFX 96TM Real-time System (Bio-Rad). qRT-PCR data were analyzed using the comparative cycle threshold (CT) method (2-ΔΔCT) in Bio-Rad CFX Maestro software. The results are presented relative to the GAPDH housekeeping gene. The primer sequences used are listed in Table 1.

NF-κB Nucleus Translocation Assay

The HeLa cell line is well documented in literature to analyze NF-κB nuclear translocation, as it has a large-sized nucleus and a flat morphology that allows easy detection of fluorescence intensity changes in the 2-D image [38]. HeLa cells were seeded in 96-well plates at 5000 cells per well in DMEM/F12 medium (Welgene, #LM002-08) supplemented with 10% FBS (YOUNG IN, US-FBS-500), 1% P-S (Gibco, 15070063) and incubated at 37 °C/5% CO$_2$ incubator. After 24 h, cells were pretreated with the drugs for 1 h and stimulated with 10 ng/ml of IL-1α

Table 1 Primers used in the qRT-PCR analysis

Primer	Forward	Reverse
GAPDH [34]	AGGTCGGTGTGAACGGATTTG	TGTAGACCATGTAGTTGAGGTCA
CCL5	CCTGCTGCTTTGCCTACCTCTC	ACACACTTGGCGGTTCCTTCGA
CD86	ACGTATTGGAAGGAGATTACAGCT	TCTGTCAGCGTTACTATCCCGC
IL-1β	TGGACCTTCCAGGATGAGGACA	GTTCATCTCGGAGCCTGTAGTG
IL-6 [35]	AGGATACCACTCCCAACAGA	ACTCCAGGTAGCTATGGTACTC
TNF-α [36]	AAATGGGCTCCCTCTCATCAGTTC	TCTGCTTGGTGGTTTGCTACGAC
iNOS	GGGCAGCCTGTGAGACCTT	TGAAGCGTTTCGGGATCTG
HB9 [37]	GAGACCCAGGTGAAGATTTG	CCTTCTGTTTCTCCGCTTCC
BDNF	CATCCGAGGACAAGGTGGCTTG	GCCGAACTTTCTGGTCCTCATC
GDNF	CCTTCGCGCTGACCAGTGACT	GCCGCTTGTTTATCTGGTGACC
NGF	ACCCGCAACATTACTGTGGACC	GACCTCGAAGTCCAGATCCTGA
IGF-1	GTGGATGCTCTTCAGTTCGTGTG	TCCAGTCTCCTCAGATCACAGC

Qiao et al. [34], Grønhøj et al. [35], Yang et al. [36], Zhang et al. [37]

(Peprotech, 200-01A) for 30 min. Cells were fixed in 10% formalin solution (Sigma, HT5011-15 ml) for 20 min and permeabilized in 0.1% TritonX-100 (Sigma, 93443). After 1 h blocking with 3% normal goat serum (CST, 5425S) and 1% bovine serum albumin (BSA) (RDT, C0082-100) in 0.2% TritonX-100 solution, cells were incubated with mouse anti- NF-κB p65 antibody (1:500, Santacruz, SC-8008) overnight at 4 °C. After washing with 0.1% TritonX-100, cells were incubated with AlexaFluor-488 conjugated anti-mouse IgG antibody (1:500, Invitrogen, A-10680) for 2 h. Nuclei were stained with DAPI (1:1000, Thermo, D1306) for 15 min. Furthermore, fluorescent images were acquired using a Cytation 5 Automated Imaging Multi-Mode reader (BioTek), and fluorescence disposition was measured using a custom-written ImageJ macrocode in the Image J software. The mean NF-κB p65 fluorescence intensity difference from the nucleus and the adjacent cytoplasm was measured to analyze fluorescence disposition.

Primary Cortical Neuronal Culture

Primary cortical neurons were prepared from pregnant C57BL/6N mice at 16 embryonic days (Koatech). For cortical neuronal culture, the brains were isolated, and the olfactory bulb and cerebellum were removed. Cortices were freed from meninges and chemically dissociated using 0.25% trypsin (Hyclone, SH-30042.01). Subsequently, the samples were gently triturated several times using a flame-polished Pasteur pipette for mechanical dissociation. Cells were cultured in Poly-D-Lysine- (Sigma, P6407) and laminin- (Corning, 354232)-coated 96-well plates (Thermo, 167008) in neurobasal™ growth media (Gibco, 21103–049) supplemented with 2 mM L-glutamine (Sigma, G7513), 1% P-S (Gibco, 15070063), and serum-free B27 (Gibco, 17504–044). The next day, 100 µl growth medium was added to each well and maintained for 3 days. The cells were used for drug experiments 5 days after the culture.

Neuronal Excitotoxicity Assay

Primary cortical neurons were plated in 96-well plates at 8 $\times 10^4$ cells per well in a growth medium and incubated in a 37 °C/5% CO_2 incubator. After 4 days, the cells were pre-treated with test drugs, including the positive control drug MK-801 (Cat.CS-0020032), purchased from AbaChem-Scene. Drugs were diluted in the treatment medium, where B27 was substituted with B27 minus antioxidants (Gibco, 10889038). After 48 h of incubation, the treatment medium containing 20 µM glutamate was added to the cells and incubated for 24 h. Cells were fixed in 10% formalin solution for 20 min and permeabilized in 0.1% TritonX-100. After 1 h blocking with 3% normal goat serum and 1% BSA in 0.2% TritonX-100 solution, the cells were incubated with

mouse anti-neuronal marker (microtubule associated protein 2, MAP2) antibody (1:5000, Milipore, MAB3418) overnight at 4 °C. After washing with 0.1% TritonX-100, samples were incubated with AlexaFluor-488 conjugated anti-mouse-IgG antibody (1:1000, Invitrogen, A-10680) for 2 h. In addition, nuclei were stained with DAPI (1:1000, Thermo, D1306) for 15 min. Fluorescent images were acquired using a Cytation 5 Automated Imaging Multi-Mode reader (BioTek), and fluorescence levels were measured using a Synergy HTX Multi-Mode reader (BioTek).

Differentiation to the Motor Neuron from NPC

ReN VM-immortalized cells were purchased from EMD Millipore (SCC008). ReN VM cells were cultured on laminin (Corning, 354232)-coated 75 T Flask in the growth medium, which is DMEM/F12 (Welgene, #LM002-08) supplemented with 20 ng/ml basic fibroblast growth factor (bFGF; Gibco, 15750-060), 20 ng/ml epidermal growth factor (EGF; Sigma, E9644), serum-free B27 (Gibco, 17504-044), 10 KU heparin (Sigma, H3393), and 1% gentamicin (Gibco, 17504-044) to sustain cell growth. Cells were plated in 96-well plates at 7000 cells per well in the growth media in a 37 °C/5% CO_2 incubator for 3 days. Subsequently, the growth medium was replaced with a differentiation medium (growth medium without bFGF and EGF), and the cells were treated with the drugs for 3 days. Immunostaining was performed against HB9, a specific motor neuronal marker, to assess the population of motor neurons. Briefly, drug-treated ReN VM cells were fixed in 10% formalin solution for 20 min and permeabilized in 0.1% TritonX-100. After incubation with Intercept® Blocking buffer (LI-COR, 927,60001) for 1 h, the cells were incubated with rabbit anti-HB9 antibody (1:300, Abcam, ab97541) overnight at 4 °C. After washing with 0.1% TritonX-100 solution, cells were incubated for 1 h with IRDye® 800 CW goat anti-rabbit IgG (1:1000, LI-COR, 925-32211) and CellTag700 (1:1000, LI-COR, 926-41090) for normalization of cell number. Fluorescence intensity levels were measured using an Odyssey® DLx Infrared Imaging System (LI-COR, CLS-2383).

In Vitro Muscle Atrophy Assay

To examine the drug's effect on muscle atrophy, a mouse myoblast cell line, namely, C2C12, was used. C2C12 cells were purchased from ATCC (CRL-1772), seeded in 96-well plates at 5×10^4 cells per well in growth medium containing 10% FBS and 1% P-S, and incubated for 24 h at 37 °C/5% CO_2 incubator. The growth medium was changed to a differentiation medium (growth medium with FBS reduced to 1%) to induce myogenic differentiation. After 4 days of differentiation, 10 ng/ml of TNF-α (R&D systems, 410-MT-010/CF) and the drug were treated for 3 days. Cells were

fixed in 10% formalin solution for 20 min and permeabilized in 0.1% TritonX-100. After 1 h with Intercept® blocking buffer (LI-COR, 927,60,001), the cells were incubated with mouse anti-myosin heavy chain (MHC) antibody (1:1000, DSHB, MF20) overnight at 4 °C. After washing with 0.1% TritonX-100 solution, cells were incubated with AlexaFluor-488 conjugated anti-mouse IgG antibody (1:1000, Invitrogen, A-10680) for 2 h. Fluorescent images were acquired using a Cytation 5 Automated Imaging Multi-Mode reader (BioTek). The ratio of MHC-positive areas in the field was measured using a custom-written ImageJ macrocode in the Image J software.

Dosing of Mice

For low-dose in vivo experiments, mice were orally administered a combination of 5 mg/kg nebivolol and 3 mg/kg donepezil at 10 weeks of age for 70 days daily. In addition, mice ($n = 20$ mice per group) were assessed for motor capabilities, and samples ($n = 10$ mice per group) of serum, spinal cord, and muscle were collected at 98 days of age for proof-of-concept studies. For high-dose experiments ($n = 12$ mice per group), 9 mg/kg nebivolol, 6 mg/kg donepezil, or their combination was orally administered from 63 days of age until the mice could not stand within 30 s. Body weight was measured once a week at 63–109 days of age and three times a week at 109 days of age until the end of the study. To determine the disease onset, mouse age (in days) when body weight decreased by more than 10% of the maximum weight was calculated. Furthermore, the date of death or euthanasia (when the endpoint was reached) was recorded for the survival analysis.

Motor Assessment

The rotarod test was conducted every week, starting at 70 days of age and continuing until day 140. Mice were given 1 day to familiarize themselves with the rotarod treadmill (JD-A-07RA5, B.S Technolab Inc., Korea) before the test by placing them on a rod rotating at 4 rpm for 5 min. In addition, mice were placed on a rod where the rotation started at 4 rpm and gradually increased to 40 rpm within 300 s to analyze motor function. The time elapsed until the mouse dropped from the rotarod was recorded.

pNF-H Chain ELISA

Serum samples ($n = 5$ mice per group) were examined for pNF-H levels using a pNF-H ELISA Kit (Arigobio, #ARG81164), according to the manufacturer's instructions. Serum samples were diluted 1:4 with dilution buffer and reacted with HRP-conjugated pNF-H antibody. The level of pNF-H was measured using a Synergy HTX Multi-Mode reader (Biotek) at 540 nm.

Immunohistochemistry and Imaging Analysis

The L2-L5 region of spinal cord samples was subjected to Nissl staining to examine the density of neurons in the spinal cord. Briefly, the samples were fixed and embedded in paraffin. Paraffin sections (thickness, 5 μm) were stained with 0.25% Cresyl Violet and dehydrated in ethanol. Nissl-stained spinal cord images were acquired under a light microscope at ×20 magnification. Large-sized (diameter ≥ 20 μm) [39, 40], Nissl-positive neurons of the ventral horn of the spinal cord were counted using a custom-written ImageJ macrocode in the ImageJ software. Two spinal cord sections were analyzed (and summed) per mouse.

To assess myofibers, TA muscle samples were subjected to laminin staining. The samples were fixed and embedded in paraffin. Cross-sections (thickness = 5 μm) were permeabilized in 0.1% TritonX-100 for 10 min. After blocking with 3% normal goat serum (Cell Signaling, 5425S) and 1% BSA in 0.2% TritonX-100 solution for 1 h, samples were incubated with rat anti-laminin-2 (α-2-chain) antibody (1:100, Enzo, #ALX-804–190-C100) overnight at 4 °C. After washing with 0.1% TritonX-100 solution, samples were incubated with anti-rat-Alexa 488(1:1000, Abcam, ab150157) for 2 h; subsequently, nuclei were stained with DAPI (1:1000, Thermo, D1306) for 10 min. Five random fields per mouse (total $n = 3$ per group) were photographed using a Lionheart LX Automated Microscope (BioTek). Cross-sectional area (CSA) of myofibers were analyzed using a custom-written ImageJ macrocode in the ImageJ software. For quantification, 400–700 myofibers per image were analyzed and a total of 6000–9000 myofibers per group were included. For myofiber distribution histogram, CSA was binned according to group (bin = 300 μm^2).

Statistical Analysis

All data were analyzed using the GraphPad Prism 9 software. Statistical significance was assessed using a one-way ANOVA or two-way ANOVA followed by Dunnett's post-hoc analysis unless otherwise noted. Kolmogorov–Smirnov test was used to assess statistical significance between cumulative distribution of myofiber CSA. All data are presented as the mean ± SEM, and significance was set at $P < 0.05$.

Results

Identification of the Combinatorial Drug

We discovered a novel combinatorial drug for ALS therapy using our proprietary AI-based screening technology (Fig. S1), establishing the pathological network using weighted correlation network analysis (WGCNA) and

calculating the probability of combinatorial drugs that can reverse the pathological subnetwork. Briefly, we constructed several subnetworks reflecting modular structures observed in many pathological phenotypes of ALS and calculated the connectivity scores (CS) between pathological modular expression and chemical-induced expression. Combinatorial drug candidates were prioritized by the final scores, quantifying the extent to which the two drugs complementarily modulate phenotype-related pathways and reverse the expression patterns of the disease. Using this novel data analysis, we identified 627 drug candidates from 1834 drugs. For the primary screening, 205 single drugs were examined for their anti-inflammatory effects and differentiation of motor neurons using BV2 cells and NPC, respectively, and 18 drugs showing tremendous significance in both assays were identified. For secondary screening, 100 different combinations of the selected single drugs were screened for their anti-inflammatory and neurogenic effects. Nebivolol and donepezil were finally selected, and further in vitro and in vivo tests were performed for validation as ALS therapies (Fig. 1).

Nebivolol and Donepezil Reduce Inflammation by Inhibiting NF-kB Nucleus Translocation

To validate the screening results, we assessed the effect of nebivolol and donepezil on neuroinflammation in vitro using a BV-2 mouse microglial cell line, which has a primary role in mediating inflammatory responses in the CNS. LPS treatment activates microglia and induces inflammatory responses, including upregulation of nitric oxide (NO) production and cytokine expression. LPS-induced microglial activation significantly increased NO production in the LPS-only treated group (LPS only) (Fig. 2a–c) compared to the untreated control group (no LPS). Nebivolol treatment at concentrations ranging from 1.25 μM to 40 μM showed a significant reduction in NO production at concentrations of 10–40 μM compared to LPS only (Fig. 2a). Considering the toxicity range of nebivolol (Fig. S2a), the reduction of NO in the 20 and 40 μM nebivolol-treated groups was due to cell death. Next, donepezil was administered at concentrations ranging from 1.25 μM to 40 μM and demonstrated a
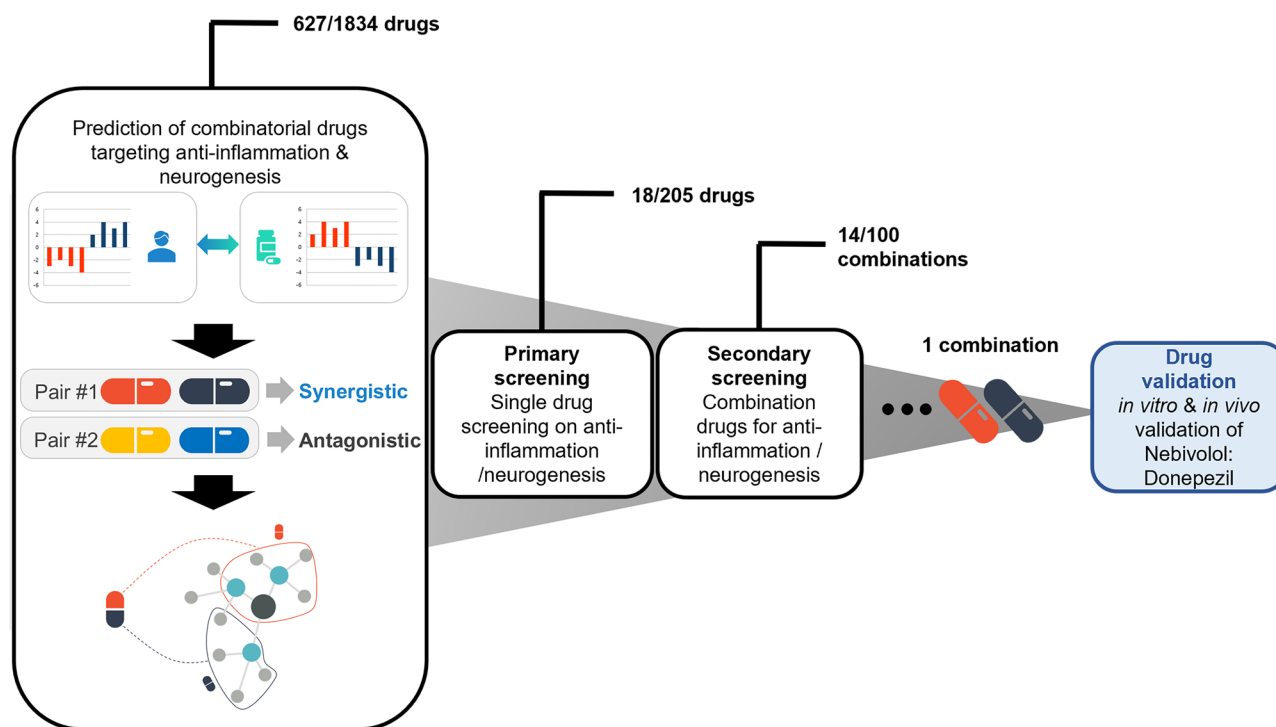

Fig. 1 The drug discovery process of the combinatorial drugs for ALS. Data analysis predicted 627 single drugs of the 1834 single drugs. Two hundred five single drugs with a high probability of the 627 in data analysis were tested for the primary screening, and 18 single drugs were effective in anti-inflammation and neurogenesis. For the secondary screening, 100 combinatorial drugs, composed of 2 single drugs showing a significant effect in primary screening were tested. Fourteen combinatorial drugs from secondary screening show an excellent effect on inflammation and neurogenesis with a synergistic effect compared to the single drugs. Finally, nebivolol-HCl and donepezil-HCl (nebivolol-donepezil) were selected, and the drugs' therapeutic effect was validated in vitro and in vivo
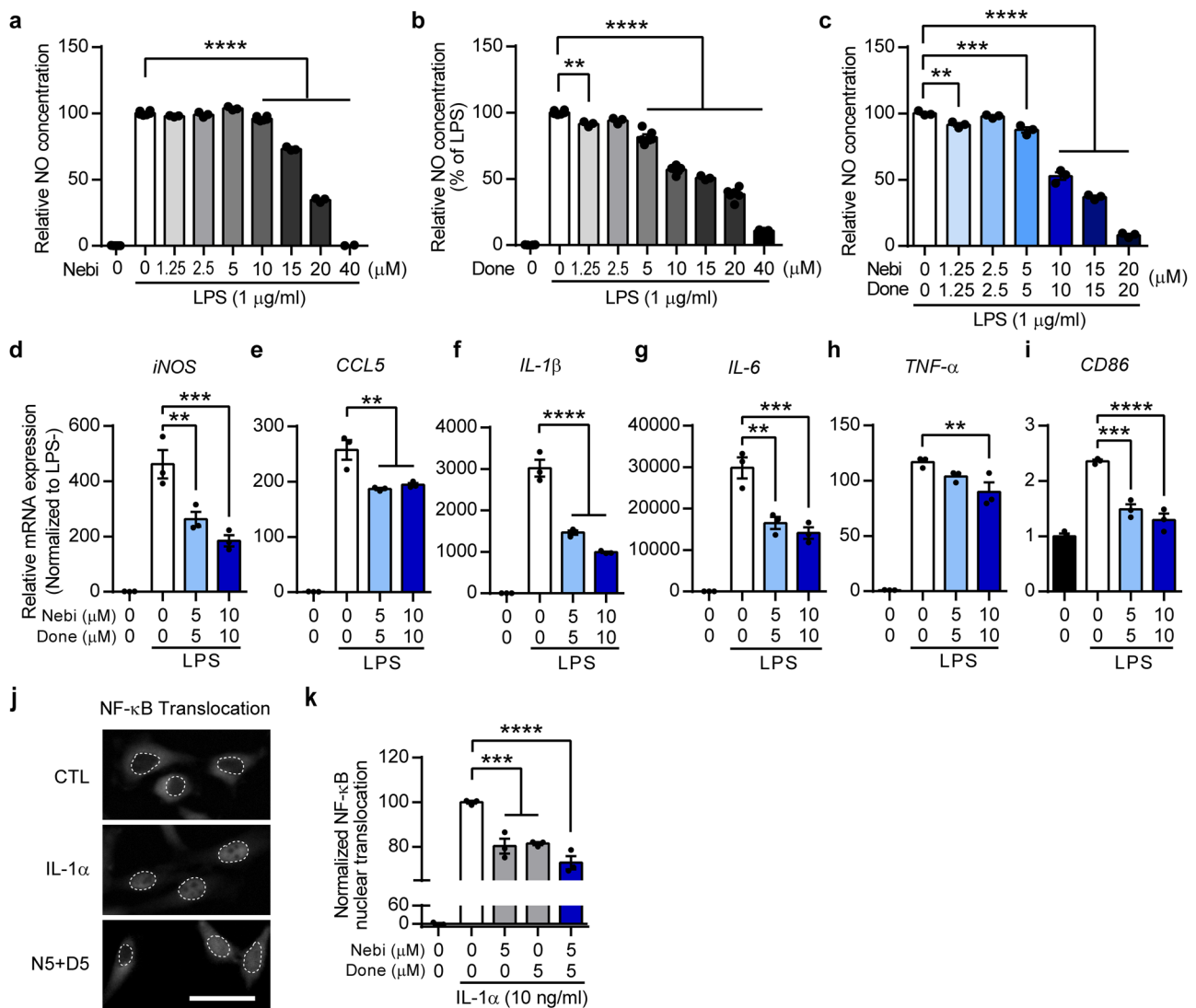
Fig. 2 Nebivolol and donepezil reduce inflammation by inhibiting NF-κB nuclear translocation. **a–c** Histograms showing a relative NO production from LPS-treated BV-2 microglia. Nebivolol (**a**), donepezil (**b**), or a 1:1 molar ratio of combination (**c**) was co-treated with LPS. NO concentration was normalized to the LPS-only-treated group (no LPS: black bar, LPS only: white bar). **d–i** Histograms showing qRT-PCR quantification results. The relative mRNA expression level of *iNOS* (**d**), *CCL5* (**e**), *IL-1β* (**f**), *IL-6* (**g**), *TNF-α* (**h**), and *CD86* (**i**) were normalized to LPS untreated control group (black bar). **j** Representa-

tive microscopic images showing the compartment of NF-κB signal in HeLa cell. The dashed line shows the boundary of the nucleus and cytoplasm. Scale bar=50 μm. **k** Histogram showing quantification result of NF-κB nuclear translocation. The mean NF-κB intensity difference between nuclear and cytoplasm was normalized to IL-1α only treated group (as 100%) and IL-1α untreated group (as 0). One-way ANOVA followed by Dunnett's post-hoc comparisons test. *$P < 0.05$, **$P < 0.01$, ***$P < 0.001$, ****$P < 0.0001$. Data are expressed as mean±SEM. Nebi=nebivolol, Done=donepezil

significant reduction in NO production at concentrations of 1.25–40 μM without affecting cell toxicity (Figs. 2b and S2b). To evaluate the anti-inflammatory effect of the combinational drug, we applied nebivolol and donepezil at a fixed ratio (1:1) of escalating doses and observed a significant attenuation of NO generation in a dose-dependent manner. The NO-reducing effect of the combinational drug was greater than the effects of every single drug of nebivolol or donepezil at the respective concentrations (Fig. 2c).

These results showed that nebivolol and/or donepezil effectively attenuated NO production in LPS-stimulated microglia, demonstrating the drug combination's efficacy in reducing neuroinflammation.

To confirm the effect of the drug combination on neuroinflammation, we evaluated the mRNA expression of inflammation-related genes. *iNOS* mRNA expression was robustly upregulated by LPS only, whereas nebivolol-donepezil treatment significantly reduced *iNOS* expression

(Fig. 2d). Considering a previous report on the role of the *iNOS* gene in NO synthesis during inflammation [41], decreased *iNOS* expression further supported the effect of nebivolol-donepezil on NO reduction. In addition, mRNA expression levels of pro-inflammatory cytokines, which are critical modulators of inflammatory responses, and *CD86*, the transmembrane protein of antigen-presenting cells that provides stimulatory signals to immune cells, were significantly decreased by treatment with the combination drug (Fig. 2e–i). These results indicate that nebivolol-donepezil effectively controlled inflammation by downregulating LPS-induced cytokines.

Previous studies have demonstrated the anti-inflammatory effects of nebivolol and donepezil via inhibition of NF-κB nuclear translocation, which mediates the transcription of inflammatory cytokines [42–44]. Therefore, we verified whether nebivolol and donepezil could inhibit the nuclear translocation of NF-κB under the effect of interleukin 1α (IL-1α). IL-1α treatment at 10 ng/ml dramatically induced NF-κB translocation to the nucleus in HeLa cells, whereas 5 μM nebivolol or donepezil significantly reduced IL-1α-induced nuclear translocation of NF-κB (Fig. 2k). Furthermore, the two drugs in combination reduced NF-κB translocation more than the single treatment with each drug (Fig. 2j, k). Collectively, these results indicate that nebivolol and donepezil exert potent anti-inflammatory effects by regulating NF-κB nuclear translocation.

Nebivolol and Donepezil Protect Neuronal Death from Excitotoxicity

One of the pathophysiological features facilitating motor neuronal loss in ALS is the excitotoxicity caused by excessive glutamate. Therefore, we investigated whether nebivolol and donepezil effectively protected neurons from glutamate-induced excitotoxicity in mouse primary cortical neuronal cultures. Treatment with 20 μM glutamate dramatically caused neuronal damage, which was examined using immunostaining for the neuronal marker MAP2. In contrast, treatment with the NMDA receptor antagonist MK801 as a positive control significantly prevented neuronal loss, consistent with previous reports (Fig. 3a–d) [45, 46]. In this system, 0.01–2.5 μM nebivolol or 0.01–10 μM donepezil dose-dependently increased neuronal survival compared to the glutamate only group, showing a protective effect of both drugs against excitotoxicity (Fig. 3a, b). In addition, combined treatment with 1 μM nebivolol and 1 μM donepezil was more protective than each drug treated alone (Fig. 3b–d).

Donepezil has been reported to elicit neuroprotective actions against excitotoxicity through PI3K-Akt signaling [47]. Therefore, we evaluated whether the protective effect of nebivolol-donepezil were PI3K-dependent. Treatment with the PI3K inhibitor LY294002 and the combination drug

significantly reversed the neuronal survival observed after treatment with the combination drug alone, indicating that nebivolol-donepezil protects neurons from excitotoxicity through the PI3K signaling pathway (Fig. 3e).

Nebivolol and Donepezil Promote the Differentiation of Motor Neurons by Increasing the Neurotrophic Factor Expression

Protection from motor neuronal death and the restoration of the neuronal population has been suggested as a vital target for therapeutic approaches for ALS treatment. ReN VM, which is an immortalized NPC line, was used to evaluate whether nebivolol and/or donepezil could accelerate the differentiation of NPC into motor neurons. Nebivolol, donepezil, and the combination of the two drugs significantly increased HB9 (a motor neuron-specific marker) expression compared to the control (Fig. 4a). We further verified that drug treatment markedly increased *HB9* mRNA levels depending on the concentration of nebivolol and/or donepezil (Fig. 4b). Several studies have demonstrated that neurotrophic factors are strongly involved in neurogenesis and neuronal differentiation [48, 49]. Next, we examined whether nebivolol and donepezil regulated the expression of neurotrophic factors. Nebivolol and donepezil markedly elevated the mRNA expression levels of neurotrophic factors: brain-derived neurotrophic factor (BDNF), glial cell-derived neurotrophic factor (GDNF), and nerve growth factor (NGF) (Fig. 4c–e). In addition, a significant increase in neurotrophic factors was observed after treatment with 1 μM nebivolol and 1 μM donepezil, consistent with HB9 protein and mRNA levels. These data indicate that nebivolol and donepezil promote motor neuronal differentiation of NPC through the upregulation of neurotrophic factor expression.

Nebivolol-Donepezil Improves Motor Function and Prevents Muscle Atrophy in ALS Mice

To evaluate the therapeutic effects of nebivolol and donepezil in an animal model of ALS, we orally administered the drugs to hSOD1^{G93A} mice for 10 weeks. First, we assessed the drug's effect on motor function using the rotarod test, which was performed weekly. The drug was administered at 70 days of age when motor deficits were not yet apparent in the transgenic mice. Normal mice (WT) showed a significant learning phase from 70 to 98 days and a steady phase from 98 to 140 days in motor coordination, whereas the TG-vehicle group (TG-Veh) showed early motor deterioration with impaired motor function during the learning phase and significantly decreased latency time during the steady phase (Fig. 5a). Nebivolol-donepezil administration (TG-N5 + D3) markedly prevented motor deficits during early disease progression, exhibiting a motor learning performance similar to
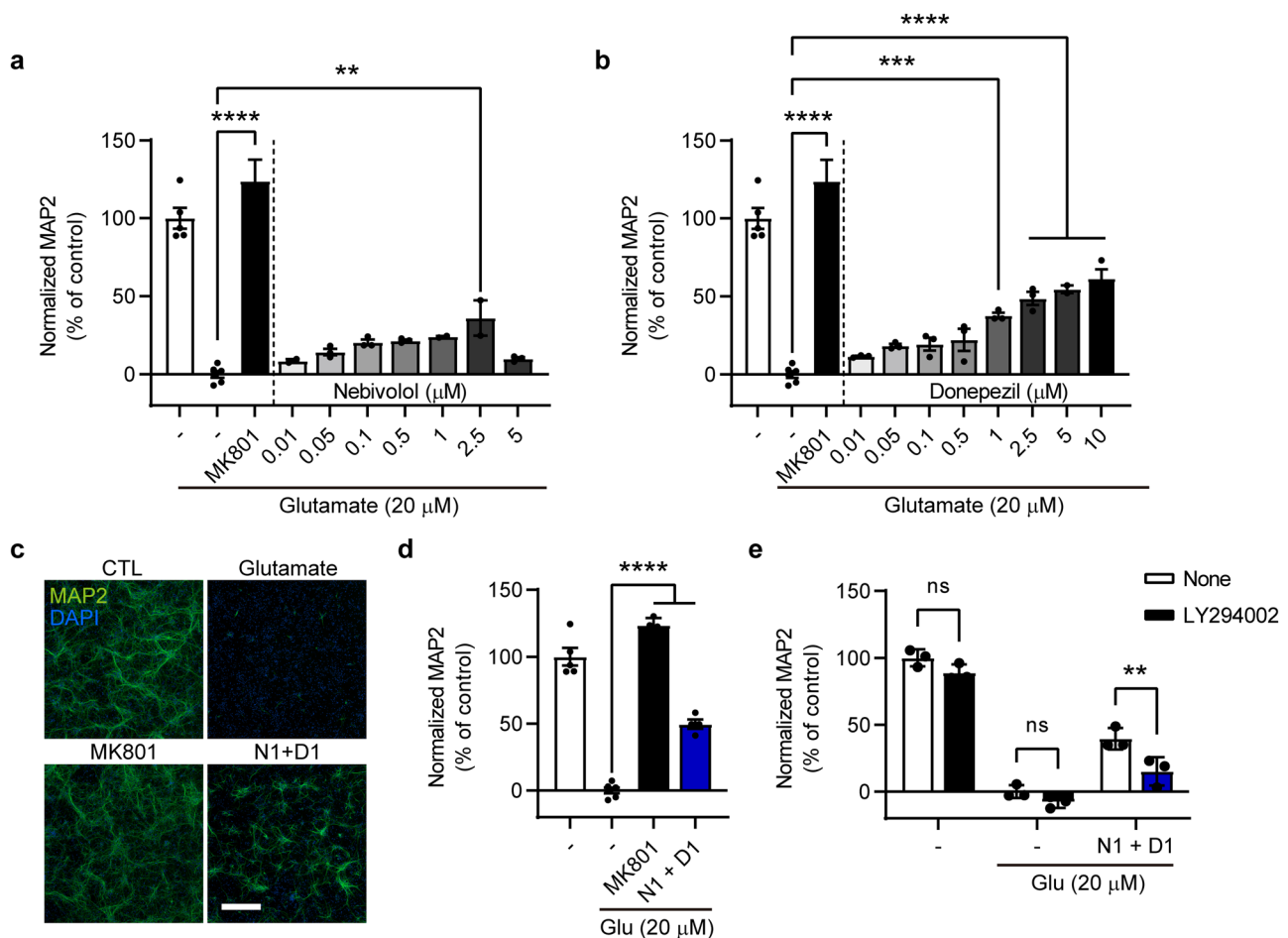
Fig. 3 Nebivolol and donepezil protect neurons from glutamate-induced excitotoxicity. (**a**, **b**, **d**, **e**) Histograms showing quantification results of relative MAP2 signal intensity. Glutamate 20 μM was treated to induce excitotoxicity in neurons. MK801, which is an NMDA receptor antagonist, was used as a positive control. Nebivolol (**a**), donepezil (**b**), combination (**d**), combination and LY294002, PI3K inhibitor (**e**), was treated to test the drug effect. MAP2 fluorescence intensity was normalized to the control groups. **c** Repre-sentative microscopic images of primary culture immunolabelled with a neuronal marker (MAP2, green) and nucleus (DAPI, blue). Scale bar = 300 μm. One-way ANOVA followed by Dunnett's post-hoc comparisons test (**a**–**d**). Two-way ANOVA followed by Sidak's post-hoc comparisons test (**e**). *$P < 0.05$, **$P < 0.01$, ***$P < 0.001$, ****$P < 0.0001$. n.s. indicates no significance. Data are expressed as mean ± SEM. N1 + D1 = nebivolol 1 μM + donepezil 1 μM

that of WT animals in the learning phase. In addition, nebiv-olol-donepezil treatment significantly increased the rotarod latency time in the steady phase compared to TG-Veh. When the rotarod performance was calibrated to the individual animal's baseline performance, the TG-Veh group showed significant impairment from day 77. In contrast, the TG-N5 + D3 group showed a similar level of decline at day 126 compared to the WT group (Fig. 5b). Therefore, drug treatment substantially delayed motor degeneration in ALS mice.

To assess whether the drug's effect on motor function is related to the prevention of motor neuronal loss, we examined the number of motor neurons in the lumbar spinal cord 28 days after nebivolol-donepezil administration. Nissl staining revealed that the number neurons in the ventral horn of TG-Veh was significantly diminished. In contrast,

the number in TG-N5 + D3 was comparable to that of WT controls, indicating that the drug treatment effectively halted the motor neuron loss during disease progression (WT:117.7 ± 6.872 cells; $n = 10$ mice, TG-Veh:64 ± 10.55 cells; $n = 6$ mice, TG-N5 + D3:181.7 ± 28.51 cells; $n = 6$ mice) (Fig. 5c, d). Moreover, we investigated the therapeutic effect of nebivolol-donepezil by measuring serum levels of the phosphorylated neurofilament heavy protein (pNF-H), a potential pharmacodynamic marker for ALS, after 28 days of drug treatment. The pNF-H levels in the TG-N5 + D3 (0.63 ± 0.2048 ng/ml, $n = 6$) were significantly lower than those in the TG-Veh (4.57 ± 1.255 ng/ml, $n = 6$) (Fig. 5e).

Muscle atrophy is one of the pathological hallmarks of ALS and is directly associated with the loss of motor neurons with innervated NMJ projecting to the muscle. Therefore,
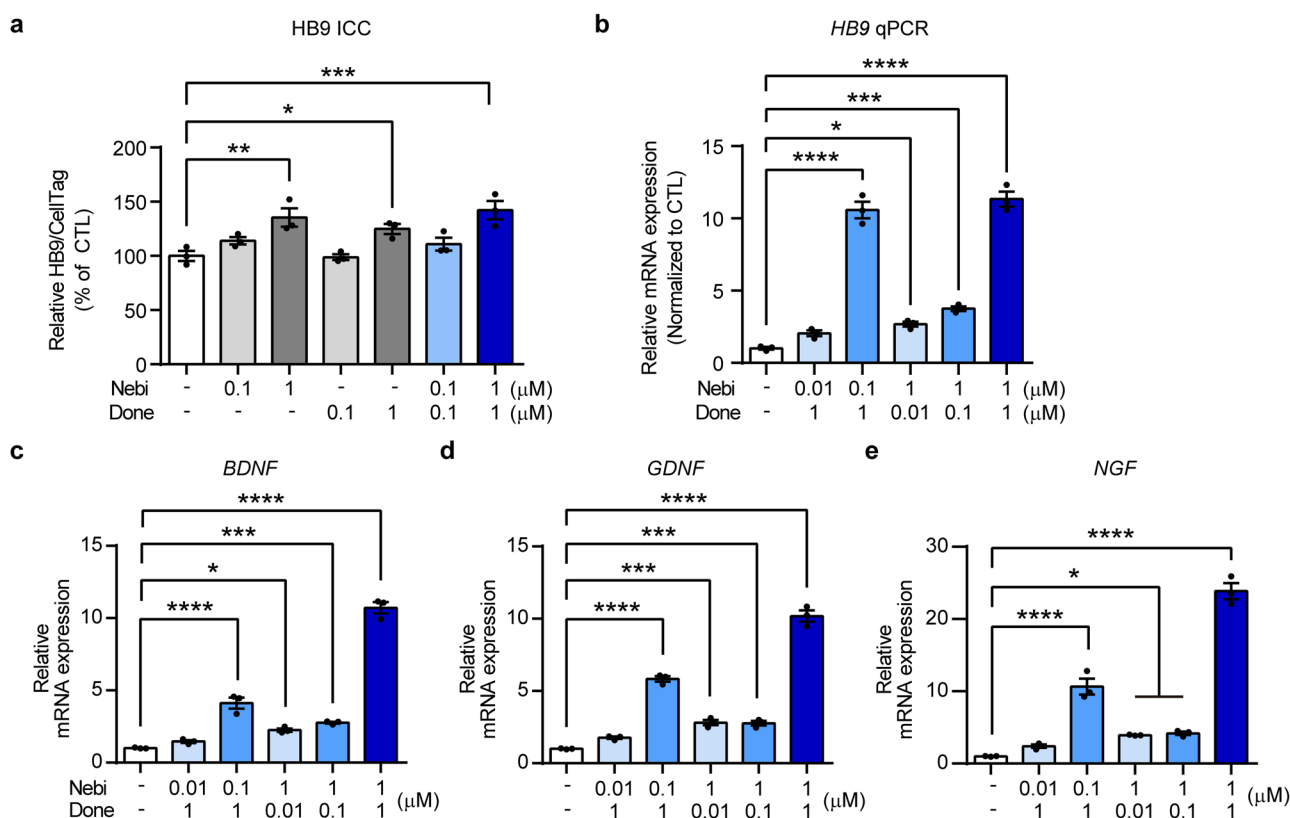
Fig. 4 Nebivolol and donepezil promote the differentiation of motor neurons by increasing neurotrophic factor expression. **a** Histogram showing immunostaining results. The HB9 expression level was normalized to the untreated control group. **b–e** Histograms showing qRT-PCR results. The relative mRNA expression levels of *HB9* (**b**), *BDNF* (**c**), *GDNF* (**d**), and *NGF* (**e**) were normalized to the untreated control group. One-way ANOVA followed by Dunnett's post-hoc comparison test. *$P < 0.05$, **$P < 0.01$, ***$P < 0.001$, ****$P < 0.0001$. Data are expressed as mean $\pm$ SEM

we further explored whether the reversal of neuronal loss in the TG-N5 + D3 group could effectively prevent muscle atrophy. The cross-section of the tibialis anterior (TA) muscle after 28 days of drug administration was immunostained against laminin, and the number and size of the myofiber cross-sectional area (CSA) were measured (Fig. 5f). Average of CSA was significantly reduced in TG groups compared to the WT group, while TG-N5 + D3 group showed significantly elevated mean CSA compared to TG-Veh group. Also, analysis of the cumulative percentage distribution of CSA of myofibers revealed a significant effect of the drug (Fig. 5g). Although there were leftward shifts in the CSA distributions for the TG groups compared to the WT group, the CSA distribution of the TG-N5 + D3 group was shifted to the right compared to that of the TG-Veh group. Previous studies have shown that the proportion of myofibers with a smaller CSA indicates muscle atrophy and is increased in SOD1^{G93A} mice [50–52]. Consistently, the TG-Veh group exhibited a remarkable increase in the proportion of smaller myofibers, ranging from 0 to 900 μm^2 of CSA, compared to the WT (Fig. 5h). However, the TG-N5 + D3 group showed a significantly reduced proportion of smaller myofibers compared to the TG-Veh group. Consequently, the overall mean CSA was significantly larger in the TG-N5 + D3 group compared to the TG-Veh group (Fig. 5i). These results suggest that nebivolol-donepezil effectively prevents muscle atrophy in the mouse model of ALS.

Nebivolol-Donepezil Significantly Delays the Disease Onset and Prolongs Survival in ALS Mice

We have demonstrated the therapeutic effects of nebivolol-donepezil on motor performance and muscle atrophy, which could positively affect the quality of life of patients with ALS. However, TG-N5 + D3 showed no effect on survival rates (Fig. S3) at low drug doses. We further verified that the high dose (N9 + D6) of drugs could effectively extend survival rates by slowing down the onset of the disease in ALS mice. To examine disease onset, administration of nebivolol-donepezil was started after the symptom of disease when the compound muscle action potential (CMAP), a feature of electrophysiology in muscle, was significantly deteriorated
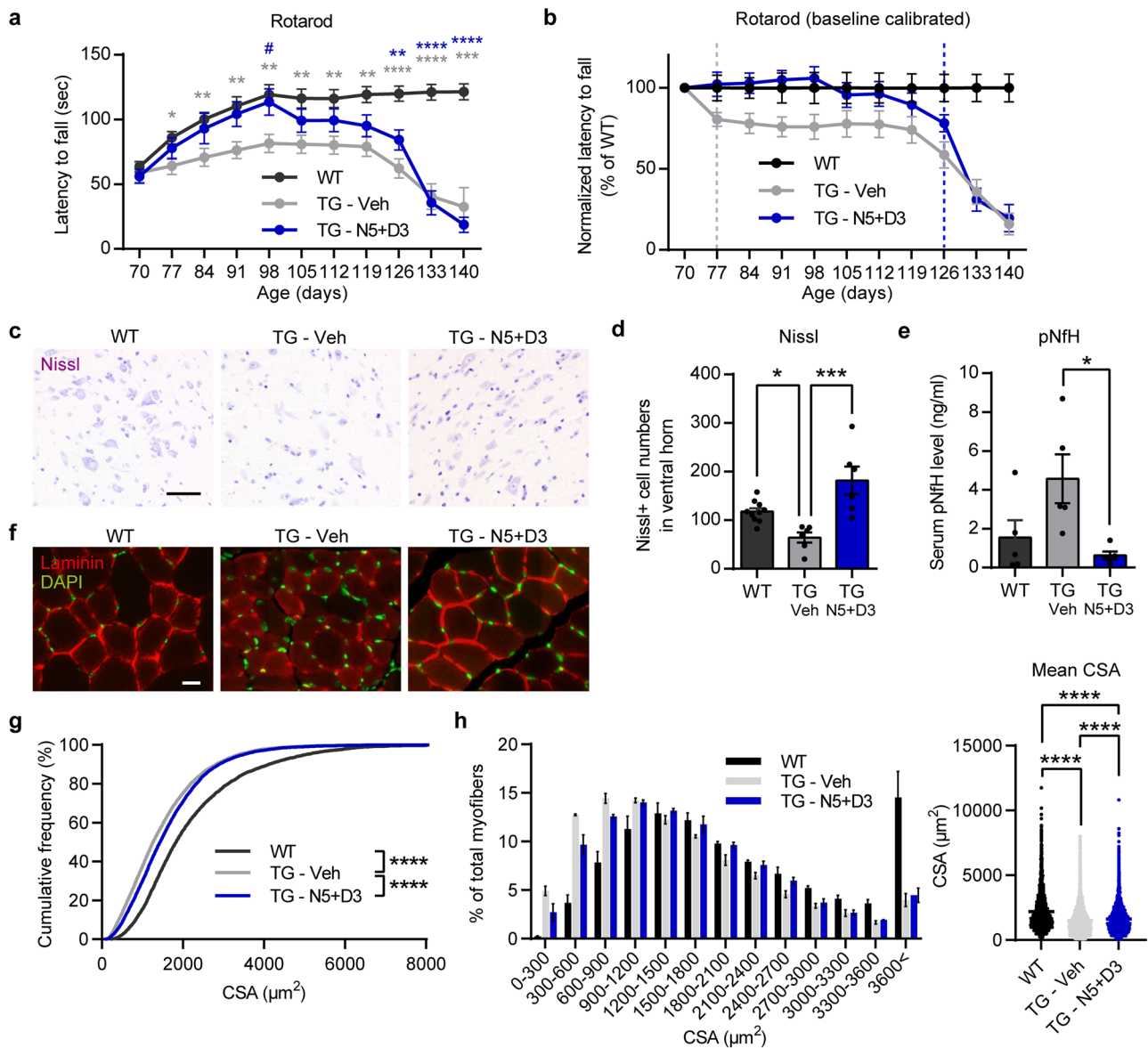
Fig. 5 Oral administration of nebivolol-donepezil improves motor function and physiological features in ALS model mice. **a** Latency to fall measured from the rotarod behavior test. The drug was orally administered from 10 weeks of age every day. The Rotarod test was performed daily. **b** Rotarod performance was calibrated to the individual animal's baseline latency (Day 70) and normalized to WT control. TG-Veh group showed a significant motor deficit from Day 77 (unpaired t-test, $P = 0.043$), while drug-treated TG showed a significant decline from Day 126 (unpaired t-test, $P = 0.042$). **c** Representative microscopic images of Nissl-stained ventral horn from wild-type, TG-Veh, and TG-N5 + D3-treated mice. Scale bar = 50 μm. **d** Quantification of the Nissl-positive motor neuron numbers in each group. **e** The concentration of pNF-H in serum from WT and

TG mice was administered with a vehicle or drug for 4 weeks. **f** Representative microscopic images of laminin-stained TA muscle from ALS model mice. Nuclei were counter-stained with DAPI (green). Scale bar = 20 μm. **g** Cumulative distribution of myofiber cross-sectional area (CSA). **h** Frequency histogram showing the distribution of myofiber CSA. Data grouped into 300 μm^2 bins. **i** Mean CSA of all myofibers analyzed. Repeated-measure two-way ANOVA followed by Tukey's post-hoc comparisons test (**a**). One-way ANOVA followed by Tukey's post-hoc comparisons test (**d**, **e**, **h**). Kolmogorov–Smirnov test (**g**). *,# $P < 0.05$, ** $P < 0.01$, *** $P < 0.001$, **** $P < 0.0001$. Compared to WT (*) or TG-Veh (#). Data are expressed as mean ± SEM. N5 + D3 = nebivolol 5 mg/kg + donepezil 3 mg/kg

compared to the WT (Fig. S4). In addition, body weight was measured to calculate the time when mice lose 10% of body weight, which is considered the onset of disease in ALS mice [53]. Administration of nebivolol-donepezil in ALS

mice significantly delayed the disease onset (when average weights were 23.2 ± 0.72 g for TG-Veh and 22.6 ± 0.38 g for TG-N9 + D6) with a time point of 70% intact mice shown at 105 days in TG-Veh compared to 117 days in TG-N9 + D6
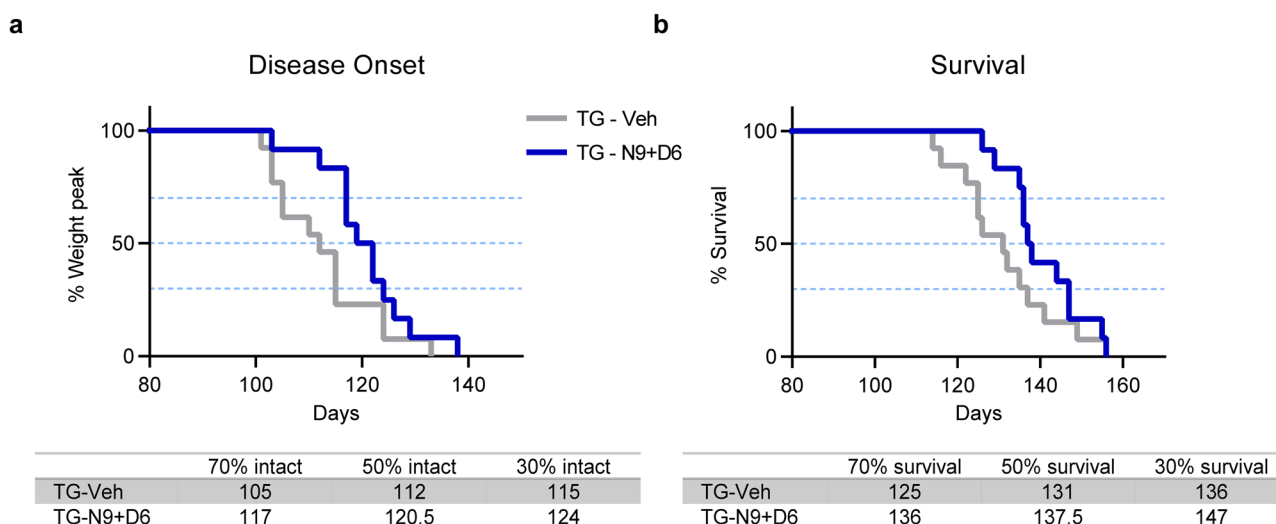
a

Disease Onset

b

Survival

	70% intact	50% intact	30% intact
TG-Veh	105	112	115
TG-N9+D6	117	120.5	124

	70% survival	50% survival	30% survival
TG-Veh	125	131	136
TG-N9+D6	136	137.5	147

Fig. 6 Oral administration of nebivolol-donepezil significantly delays disease onset and prolongs survival in ALS mice. **a** The onset of disease was scored as the percentage of animals losing 10% of peak body weight. $P = 0.0331$ by Gehan-Breslow-Wilcoxon test. **b**

Kaplan–Meier survival curves of vehicle-treated ($n = 13$ mice) and drug-treated ALS mice ($n = 12$ mice). $P = 0.0417$ by Gehan–Breslow-Wilcoxon test

(Fig. 6a). Finally, we evaluated whether the effects of nebivolol-donepezil on disease onset could extend the survival rates of ALS mice. Administration of nebivolol-donepezil significantly prolonged the survival by extending survival by 11 days (the time point of 70% survival probability was 125 and 136 days in TG-Veh and TG-N9 + D6, respectively) (Fig. 6b). However, each high dose-single compound-treated group had no beneficial effect on disease onset and survival compared to the TG-Veh group (Fig. S5).

Overall, these data indicate that administration of nebivolol-donepezil notably prolongs survival and delays disease onset in ALS mice, suggesting the combined drug's efficacy in patients' life span and not only their quality of life.

Discussion

Over the past few decades, a multitude of experimental drugs have been shown to halt disease progression in preclinical animal models of ALS. However, most studies failed to show similar levels of efficacy in human clinical trials [54–57]. The reasons for the discrepancy between preclinical and clinical trials are: various, yet different, causes of the disease and heterogeneity among patients. In addition, our in vivo efficacy with combinational drugs is also restricted to the SOD1 mutant, whereas ALS possesses greater genetic complexity. Although an extensive study of all the genetic models may not be possible, developing a multitargeting drug that can resolve ALS symptoms regardless of genetic background may overcome the failure in clinical trials and lead to more innovative opportunities to cure ALS.

In addition, previous drug development targeting one mechanism for ALS therapy could increase the failure in clinical trials or could not overcome the prominent therapeutic effect in patients with ALS. The mechanisms of action (MOA) of previous FDA-approved drugs for ALS, namely, riluzole and edaravone, are relatively restricted or unknown. Riluzole is a glutamate antagonist predicted to help patients through its anti-excitotoxic effects [58–60], whereas the only estimated mechanism of edaravone is anti-oxidation [61–63]. The single-targeting properties of riluzole and edaravone limit their efficacy in increasing survival by a short period or in patients with milder symptoms and shorter disease duration [57].

Recently, the combined administration of sodium phenylbutyrate and taurursodiol received FDA approval because of the drug's ability to target multiple processes implicated in the pathophysiology of ALS (NCT03127514). Phenylbutyrate-taurursodiol was reported to reduce neuronal cell death by mitigating endoplasmic reticulum stress and mitochondrial dysfunction [64]. This successful trial increases the rationale for drug development by multitargeting ALS pathophysiology. Our extensive in vitro and in vivo data demonstrated the diverse MOAs of our combinatorial drug against ALS, providing sufficient evidence for nebivolol-donepezil to advance further clinical investigations.

Benefiting from AI-based drug screening, nebivolol-donepezil was identified for ALS therapy. Here, we describe a novel drug combination that effectively targets the multifactorial mechanisms related to ALS (Fig. 7). We suggest four different MOAs for the therapeutic effect of nebivolol-donepezil: anti-inflammation, neuroprotection, neurogenesis, and muscle atrophy prevention.

Fig. 7 Mechanism of action of nebivolol and donepezil. AchR = acetylcholine receptor; β2AR = beta-2 adrenergic receptor
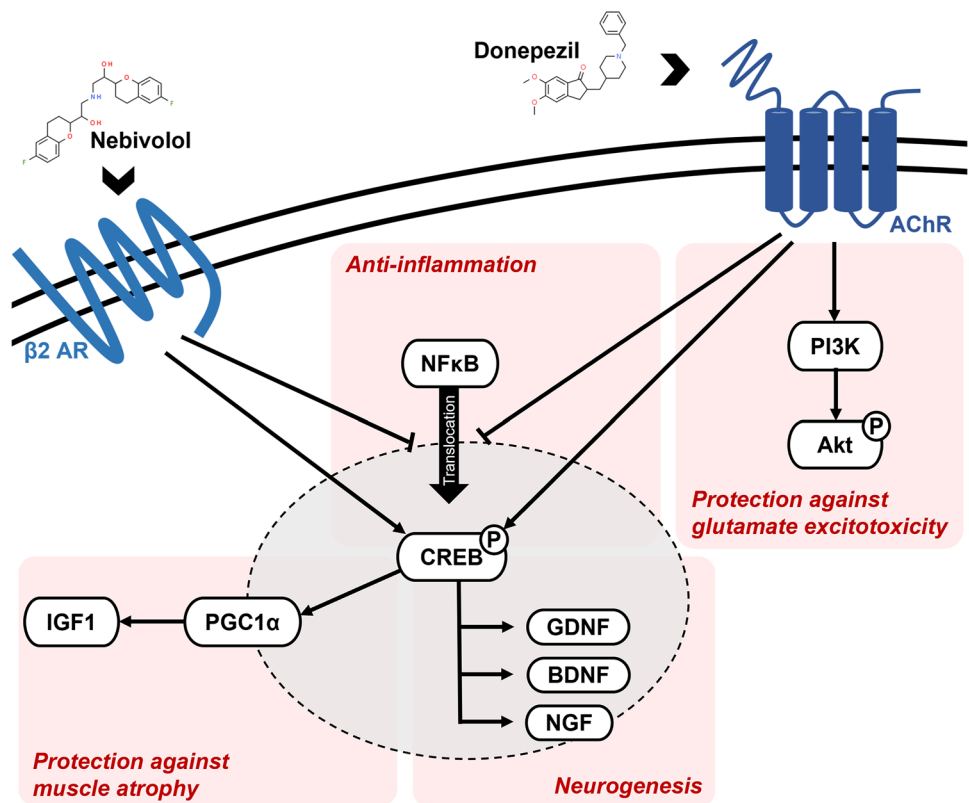
Neuroinflammation is one of the most striking pathological findings of ALS shared by familial and sporadic patients and is characterized by extensive microglial activation, astrogliosis, and infiltration of monocytes and T-cells [65–69]. However, attempts to eliminate downstream inflammatory genes in ALS animal models are not helpful [70, 71] or even detrimental [72], emphasizing the complexity of neuroinflammation in ALS. A more successful approach would target the upstream transcription factors responsible for inflammation, such as NF-κB. The nuclear factor is a major regulator of microglial inflammation [73] and is upregulated in the spinal cords of patients with ALS and ALS model mice [74]. Constitutive activation of NF-κB in microglia induces gliosis and motor neuronal death in vitro and in vivo, providing a therapeutic target for modulating the progression of ALS [75]. Studies have demonstrated that adrenergic and cholinergic signaling are associated with regulating microglial inflammation by inhibiting NF-κB nuclear translocation [42–44]. Consistently, we found reduced compartmentalization of NF-κB in the nucleus of HeLa cells following treatment with nebivolol (partial adrenergic agonist), donepezil (acetylcholinesterase inhibitor), or nebivolol-donepezil. Deletion of NF-κB signaling and the resultant alleviation of inflammatory responses are known to rescue motor neurons from microglial-mediated death and extend survival in ALS mice [75], which was also demonstrated by our in vivo results.

The glutamate hypothesis is a well-established pathophysiological mechanism of motor neuron injury in ALS [20]. Due to their low endogenous calcium buffering capacity, spinal and brainstem motor neurons are particularly vulnerable to excessive glutamate, which disrupts muscle calcium homeostasis [76, 77]. Interference of glutamate-mediated excitotoxicity is one of the few neuroprotective strategies that has slowed disease progression in patients with ALS [78]. Treatment with nebivolol-donepezil demonstrated a PI3K-dependent increase in neuronal viability under glutamate excitotoxicity, thereby expanding the therapeutic capacity of the drug in ALS mice.

Increased expression of neurotrophins is strongly associated with anti-apoptosis, neuroprotection, and neurogenesis [79, 80]. Multiple factors, including BDNF, ciliary neurotrophic factor (CNTF), GDNF, IGF-1, and granulocyte colony-stimulating factor, have been investigated in preclinical models of ALS [8]. The administration of neurotrophic factors remarkably affects the survival of degenerating motor neurons in rodent ALS models [81]. Additionally, BDNF [82], CNTF [83], and IGF-1 [84–86] have been examined in large-scale human clinical trials. Therefore, elevated expression of neurotrophins, including BDNF, GDNF, and NGF, along with increased differentiation of NPC to motor neurons by nebivolol-donepezil treatment, were likely translated in vivo as protection from spinal cord motor neuronal loss and extended lifespan of SOD1 mice.

Numerous studies have shown that increased levels of insulin growth factor-1 (IGF-1) stimulate protein synthesis and attenuate protein degradation in skeletal muscle, which promotes muscle growth [87–89]. Using differentiated C2C12 myocytes, we observed significant upregulation of *IGF-1* mRNA levels following nebivolol and donepezil treatment (Fig. S6a). In turn, we verified that the drug effectively protected C2C12 cells from both tumor necrosis factor-α (TNF-α)-induced atrophy (Fig. S6b). We suspect a similar IGF-1-inducing mechanism was triggered in vivo, that converted to improved myofiber health in the ALS animal model. Furthermore, IGF-1 overexpression improves muscle function and extends the lifespan of mice suffering from different types of muscle diseases [90, 91]. Therefore, the IGF-1-inducing effect of our drug likely has a beneficial influence on rotarod performance, weight loss, and survival.

In conclusion, a multitargeting approach using a combinational drug, nebivolol-donepezil, effectively delays disease onset, including motor degeneration and motor neuronal loss, and extends survival. Among the recently growing number of clinical trials with combinational drugs for CNS disorders, the multifactorial targeting drug nebivolol-donepezil could provide therapeutic potential for patients with ALS.

Author Contributions EJK and JHL designed and supervised the research. SYL, HP and JPO performed the experiments. EJK, SYL, HYC, JPO and JP analyzed data. SHB coded the deep learning software to analyze gene expression data. EJK, HYC, SYL, JPO, JP, SHB and JHL wrote the manuscript. All authors have read and approved the final version of the manuscript.

Data Availability The data reported in this paper is available from the lead contact upon reasonable request.

Declarations

Conflict of Interest SYL, HYC, JPO, JP, SHB, HP, EJK are employees of DR. NOAH BIOTECH Inc. JHL is the founder and CEO of DR. NOAH BIOTECH Inc. EJK and JHL are inventors on multiple patents that disclose nebivolol and donepezil and their related compounds as ALS therapeutics.

References

1. Mitchell JD, Borasio GD. Amyotrophic lateral sclerosis. Lancet. 2007;369(9578):2031–41. https://doi.org/10.1016/S0140-6736(07)60944-1.

2. Scott A. Drug therapy: on the treatment trail for ALS. Nature. 2017;550(7676):S120–1. https://doi.org/10.1038/550S120a.

3. Kumar V, Islam A, Hassan MI, et al. Therapeutic progress in amyotrophic lateral sclerosis-beginning to learning. Eur J Med Chem. 2016;121:903–17. https://doi.org/10.1016/j.ejmech.2016.06.017.

4. Gordon P, Corcia P, Meininger V. New therapy options for amyotrophic lateral sclerosis. Expert Opin Pharmacother. 2013;14(14):1907–17. https://doi.org/10.1517/14656566.2013.819344.

5. Wright AL, Della Gatta PA, Le S, et al. Riluzole does not ameliorate disease caused by cytoplasmic TDP-43 in a mouse model of amyotrophic lateral sclerosis. Eur J Neurosci. 2021;54(6):6237–55. https://doi.org/10.1111/ejn.15422.

6. Witzel S, Maier A, Steinbach R, et al. Safety and effectiveness of long-term intravenous administration of edaravone for treatment of patients with amyotrophic lateral sclerosis. JAMA Neurol. 2022;79(2):121–30. https://doi.org/10.1001/jamaneurol.2021.4893.

7. Blackburn D, Sargsyan S, Monk PN, et al. Astrocyte function and role in motor neuron disease: a future therapeutic target? Glia. 2009;57(12):1251–64. https://doi.org/10.1002/glia.20848.

8. Henriques A, Pitzer C, Schneider A. Neurotrophic growth factors for the treatment of amyotrophic lateral sclerosis: where do we stand? Front Neurosci. 2010;4:32. https://doi.org/10.3389/fnins.2010.00032.

9. Liu J, Wang F. Role of neuroinflammation in amyotrophic lateral sclerosis: Cellular mechanisms and therapeutic implications. Front Immunol. 2017;8:1005. https://doi.org/10.3389/fimmu.2017.01005.

10. Tortelli R, Zecca C, Piccininni M, et al. Plasma inflammatory cytokines are elevated in ALS. Front Neurol. 2020;11:552295. https://doi.org/10.3389/fneur.2020.552295.

11. Hu Y, Cao C, Qin XY, et al. Increased peripheral blood inflammatory cytokine levels in amyotrophic lateral sclerosis: a meta-analysis study. Sci Rep. 2017;7:9094. https://doi.org/10.1038/s41598-017-09097-1.

12. Fischer LR, Culver DG, Tennant P, et al. Amyotrophic lateral sclerosis is a distal axonopathy: evidence in mice and man. Exp Neurol. 2004;185(2):232–40. https://doi.org/10.1016/j.expneurol.2003.10.004.

13. Cappello V, Francolini M. Neuromuscular junction dismantling in amyotrophic lateral sclerosis. Int J Mol Sci. 2017. https://doi.org/10.3390/ijms18102092.

14. Collard JF, Cote F, Julien JP. Defective axonal transport in a transgenic mouse model of amyotrophic lateral sclerosis. Nature. 1995;375(6526):61–4. https://doi.org/10.1038/375061a0.

15. Strom AL, Gal J, Shi P, et al. Retrograde axonal transport and motor neuron disease. J Neurochem. 2008;106(2):495–505. https://doi.org/10.1111/j.1471-4159.2008.05393.x.

16. Dupuis L, Gonzalez de Aguilar JL, Oudart H, et al. Mitochondria in amyotrophic lateral sclerosis: a trigger and a target. Neurodegener Dis. 2004;1(6):245–54. https://doi.org/10.1159/000085063.

17. Bacman SR, Bradley WG, Moraes CT. Mitochondrial involvement in amyotrophic lateral sclerosis: trigger or target? Mol Neurobiol. 2006;33(2):113–31. https://doi.org/10.1385/MN:33:2:113.

18. Martin LJ. Mitochondriopathy in Parkinson disease and amyotrophic lateral sclerosis. J Neuropathol Exp Neurol. 2006;65(12):1103–10. https://doi.org/10.1097/01.jnen.0000248541.05552.c4.

19. Kinoshita Y, Ito H, Hirano A, et al. Nuclear contour irregularity and abnormal transporter protein distribution in anterior horn cells in amyotrophic lateral sclerosis. J Neuropathol Exp Neurol. 2009;68(11):1184–92. https://doi.org/10.1097/NEN.0b013e3181bc3bec.

20. Shaw PJ, Ince PG. Glutamate, excitotoxicity and amyotrophic lateral sclerosis. J Neurol. 1997;244(Suppl 2):S3-14. https://doi.org/10.1007/BF03160574.

21. Corona JC, et al. Glutamate excitotoxicity and therapeutic targets for amyotrophic lateral sclerosis. Expert Opin Ther Targets. 2007;11(11):1415–28. https://doi.org/10.1517/14728222.11.11.1415.

22. Carter BJ, Anklesaria P, Choi S, et al. Redox modifier genes and pathways in amyotrophic lateral sclerosis. Antioxid Redox Signal. 2009;11(7):1569–86. https://doi.org/10.1089/ars.2008.2414.

23. Edgar R, Domrachev M, Lash AE. Gene Expression Omnibus: NCBI gene expression and hybridization array data repository. Nucleic Acids Res. 2002;30(1):207–10. https://doi.org/10.1093/nar/30.1.207.

24. Dafinca R, Scaber J, Ababneh N, et al. C9orf72 hexanucleotide expansions are associated with altered endoplasmic reticulum calcium homeostasis and stress granule formation in induced pluripotent stem cell-derived neurons from patients with amyotrophic lateral sclerosis and frontotemporal dementia. Stem Cells. 2016;34(8):2063–78. https://doi.org/10.1002/stem.2388.

25. Fujimori K, Ishikawa M, Otomo A, et al. Modeling sporadic ALS in iPSC-derived motor neurons identifies a potential therapeutic agent. Nat Med. 2018;24(10):1579–89. https://doi.org/10.1038/s41591-018-0140-5.

26. Rabin SJ, Kim JM, Baughn M, et al. Sporadic ALS has compartment-specific aberrant exon splicing and altered cell-matrix adhesion biology. Hum Mol Genet. 2010;19(2):313–28. https://doi.org/10.1093/hmg/ddp498.

27. Kirby J, Ning K, Ferraiuolo L, et al. Phosphatase and tensin homologue/protein kinase B pathway linked to motor neuron survival in human superoxide dismutase 1-related amyotrophic lateral sclerosis. Brain. 2011;134(Pt 2):506–17. https://doi.org/10.1093/brain/awq345.

28. Highley JR, Kirby J, Jansweijer JA, et al. Loss of nuclear TDP-43 in amyotrophic lateral sclerosis (ALS) causes altered expression of splicing machinery and widespread dysregulation of RNA splicing in motor neurones. Neuropathol Appl Neurobiol. 2014;40(6):670–85. https://doi.org/10.1111/nan.12148.

29. Cooper-Knock J, Bury JJ, Heath PR, et al. C9ORF72 GGGGCC expanded repeats produce splicing dysregulation which correlates with disease severity in amyotrophic lateral sclerosis. PLoS ONE. 2015;10(5):e0127376. https://doi.org/10.1371/journal.pone.0127376.

30. Sareen D, O'Rourke JG, Meera P, et al. Targeting RNA foci in iPSC-derived motor neurons from ALS patients with a C9ORF72 repeat expansion. Sci Transl Med. 2013;5(208):208ra149. https://doi.org/10.1126/scitranslmed.3007529.

31. Langfelder P, Horvath S. WGCNA: an R package for weighted correlation network analysis. BMC Bioinformatics. 2008;9:559. https://doi.org/10.1186/1752-0509-1-54.

32. Subramanian A, Narayan R, Corsello SM, et al. A next generation connectivity map: L1000 platform and the first 1,000,000 profiles. Cell. 2017;171(6):1437–52.e17. https://doi.org/10.1016/j.cell.2017.10.049.

33. Lamb J, Crawford ED, Peck D, et al. The Connectivity Map: using gene-expression signatures to connect small molecules, genes, and disease. Science. 2006;313(5795):1929–35. https://doi.org/10.1126/science.1132939.

34. Qiao J, Zhao J, Chang S, et al. MicroRNA-153 improves the neurogenesis of neural stem cells and enhances the cognitive ability of aged mice through the notch signaling pathway. Cell Death Differ. 2020;27(2):808–25. https://doi.org/10.1038/s41418-019-0388-4.

35. Grønhøj MH, Clausen BH, Fenger CD, et al. Beneficial potential of intravenously administered IL-6 in improving outcome after murine experimental stroke. Brain Behav Immun. 2017;65:296–311. https://doi.org/10.1016/j.bbi.2017.05.019.

36. Yang M, Lin HB, Gong S, et al. Effect of Astragalus polysaccharides on expression of TNF-α, IL-1β and NFATc4 in a rat model of experimental colitis. Cytokine. 2014;70(2):81–6. https://doi.org/10.1016/j.cyto.2014.07.250.

37. Zhang Y, Wang J, Chen G, et al. Inhibition of Sirt1 promotes neural progenitors toward motoneuron differentiation from human embryonic stem cells. Biochem Biophys Res Commun. 2011;404(2):610–4. https://doi.org/10.1016/j.bbrc.2010.12.014.

38. Trask OJ Jr. Nuclear Factor Kappa B (NF-κB) translocation assay development and validation for high content screening. In: Assay guidance manual [Internet]. Bethesda (MD): Eli Lilly & Company and the National Center for Advancing Translational Sciences; 2012.

39. Hilton J, Mercer S, Lim N, et al. Cu^{II}(atsm) improves the neurological phenotype and survival of SOD1G93A mice and selectively increases enzymatically active SOD1 in the spinal cord. Sci Rep. 2017;7:42292. https://doi.org/10.1038/srep42292.

40. Turner BJ, Alfazema N, Sheean RK, et al. Overexpression of survival motor neuron improves neuromuscular function and motor neuron survival in mutant SOD1 mice. Neurobiol Aging. 2014;35(4):906–15. https://doi.org/10.1016/j.neurobiolaging.2013.09.030.

41. Arias-Salvatierra D, Silbergeld EK, Acosta-Saavedra LC, et al. Role of nitric oxide produced by iNOS through NF-κB pathway in migration of cerebellar granule neurons induced by Lipopolysaccharide. Cell Signal. 2011;23(2):425–35. https://doi.org/10.1016/j.cellsig.2010.10.017.

42. Ryan KJ, Griffin E, Yssel JD, et al. Stimulation of central β2-adrenoceptors suppresses NF-κB activity in rat brain: a role for I-κB. Neurochem Int. 2013;63(5):368–78. https://doi.org/10.1016/j.neuint.2013.07.006.

43. Kim J, Lee HJ, Park SK, et al. Donepezil regulates LPS and Aβ-stimulated neuroinflammation through MAPK/NLRP3 inflammasome/STAT3 signaling. Int J Mol Sci. 2021. https://doi.org/10.3390/ijms221910637.

44. Xia Y, Wu Q, Mak S, et al. Regulation of acetylcholinesterase during the lipopolysaccharide-induced inflammatory responses in microglial cells. FASEB J. 2022;36(3):e22189. https://doi.org/10.1096/fj.202101302RR.

45. Weller M, Marini AM, Finiels-Marlier F, et al. MK-801 and memantine protect cultured neurons from glutamate toxicity induced by glutamate carboxypeptidase-mediated cleavage of methotrexate. Eur J Pharmacol. 1993;248(4):303–12. https://doi.org/10.1016/0926-6917(93)90004-a.

46. Berman FW, Murray TF. Characterization of [3H]MK-801 binding to N-methyl-D-aspartate receptors in cultured rat cerebellar granule neurons and involvement in glutamate-mediated toxicity. J Biochem Toxicol. 1996;11(5):217–26. https://doi.org/10.1002/(SICI)1522-7146(1996)11:5%3c217::AID-JBT2%3e3.0.CO;2-N.

47. Asomugha CO, Linn DM, Linn CL. ACh receptors link two signaling pathways to neuroprotection against glutamate-induced excitotoxicity in isolated RGCs. J Neurochem. 2010;112(1):214–26. https://doi.org/10.1111/j.1471-4159.2009.06447.x.

48. Vilar M, Mira H. Regulation of neurogenesis by neurotrophins during adulthood: Expected and unexpected roles. Front Neurosci. 2016;10:26. https://doi.org/10.3389/fnins.2016.00026.

49. Shohayeb B, Diab M, Ahmed M, et al. Factors that influence adult neurogenesis as potential therapy. Transl Neurodegener. 2018;7:4. https://doi.org/10.1186/s40035-018-0109-9.

50. Kook MG, Lee S, Shin N, et al. Repeated intramuscular transplantations of hUCB-MSCs improves motor function and survival in the SOD1G(93)A mice through activation of AMPK. Sci Rep. 2020;10(1):1572. https://doi.org/10.1038/s41598-020-58221-1.

51. Dobrowolny G, Aucello M, Rizzuto E, et al. Skeletal muscle is a primary target of SOD1G93A-mediated toxicity. Cell Metab. 2008;8(5):425–36. https://doi.org/10.1016/j.cmet.2008.09.002.

52. Miyoshi S, Tezuka T, Arimura S, et al. DOK7 gene therapy enhances motor activity and life span in ALS model mice. EMBO Mol Med. 2017;9(7):880–9. https://doi.org/10.15252/emmm.201607298.

53. McCampbell A, Cole T, Wegener AJ, et al. Antisense oligonucleotides extend survival and reverse decrement in muscle response in ALS models. J Clin Invest. 2018;128(8):3558–67. https://doi.org/10.1172/JCI99081.

54. Petrov D, Mansfield C, Moussy A, et al. ALS clinical trials review: 20 years of failure. Are we any closer to registering a new treatment? Front Aging Neurosci. 2017;9:68. https://doi.org/10.3389/fnagi.2017.00068.

55. Bhandari R, Kuhad A, Kuhad A. Edaravone: a new hope for deadly amyotrophic lateral sclerosis. Drugs Today (Barc). 2018;54(6):349–60. https://doi.org/10.1358/dot.2018.54.6.2828189.

56. Ortiz JF, Khan SA, Salem A, et al. Post-marketing experience of edaravone in amyotrophic lateral sclerosis: a clinical perspective and comparison with the clinical trials of the drug. Cureus. 2020;12(10):e10818. https://doi.org/10.7759/cureus.10818.

57. Jaiswal MK. Riluzole and edaravone: a tale of two amyotrophic lateral sclerosis drugs. Med Res Rev. 2019;39(2):733–48. https://doi.org/10.1002/med.21528.

58. Kretschmer BD, Kratzer U, Schmidt WJ. Riluzole, a glutamate release inhibitor, and motor behavior. Naunyn Schmiedebergs Arch Pharmacol. 1998;358(2):181–90. https://doi.org/10.1007/pl00005241.

59. Frizzo ME, Dall'Onder LP, Dalcin KB, et al. Riluzole enhances glutamate uptake in rat astrocyte cultures. Cell Mol Neurobiol. 2004;24(1):123–8. https://doi.org/10.1023/b:cemn.0000012717.37839.07.

60. Doble A. The pharmacology and mechanism of action of riluzole. Neurology. 1996;47(6 Suppl 4):S233–41. https://doi.org/10.1212/wnl.47.6_suppl_4.233s.

61. Nagase M, Yamamoto Y, Miyazaki Y, et al. Increased oxidative stress in patients with amyotrophic lateral sclerosis and the effect of edaravone administration. Redox Rep. 2016;21(3):104–12. https://doi.org/10.1179/1351000215Y.0000000026.

62. Ohta Y, Nomura E, Shang J, et al. Enhanced oxidative stress and the treatment by edaravone in mice model of amyotrophic lateral sclerosis. J Neurosci Res. 2019;97(5):607–19. https://doi.org/10.1002/jnr.24368.

63. Nakanishi T, Tsujii M, Asano T, et al. Protective effect of edaravone against oxidative stress in C2C12 myoblast and impairment of skeletal muscle regeneration exposed to ischemic injury in ob/ob mice. Front Physiol. 2019;10:1596. https://doi.org/10.3389/fphys.2019.01596.

64. Fels JA, Dash J, Leslie K, et al. Effects of PB-TURSO on the transcriptional and metabolic landscape of sporadic ALS fibroblasts. Ann Clin Transl Neurol. 2022;9(10):1551–64. https://doi.org/10.1002/acn3.51648.

65. Alexianu ME, Kozovska M, Appel SH. Immune reactivity in a mouse model of familial ALS correlates with disease progression. Neurology. 2001;57(7):1282–9. https://doi.org/10.1212/wnl.57.7.1282.

66. Hall ED, Oostveen JA, Gurney ME. Relationship of microglial and astrocytic activation to disease onset and progression in a transgenic model of familial ALS. Glia. 1998;23(3):249–56. https://doi.org/10.1002/(sici)1098-1136(199807)23:3%3c249::aid-glia7%3e3.0.co;2-#.

67. Kawamata T, Akiyama H, Yamada T, et al. Immunologic reactions in amyotrophic lateral sclerosis brain and spinal cord tissue. Am J Pathol. 1992;140(3):691–707.

68. Mantovani S, Garbelli S, Pasini A, et al. Immune system alterations in sporadic amyotrophic lateral sclerosis patients suggest an ongoing neuroinflammatory process. J Neuroimmunol. 2009;210(1–2):73–9. https://doi.org/10.1016/j.jneuroim.2009.02.012.

69. Turner MR, Cagnin A, Turkheimer FE, et al. Evidence of widespread cerebral microglial activation in amyotrophic lateral sclerosis: an [11C](R)-PK11195 positron emission tomography study. Neurobiol Dis. 2004;15(3):601–9. https://doi.org/10.1016/j.nbd.2003.12.012.

70. Son M, Fathallah-Shaykh HM, Elliott JL. Survival in a transgenic model of FALS is independent of iNOS expression. Ann Neurol. 2001;50(2):273. https://doi.org/10.1002/ana.1104.

71. Almer G, Kikuchi H, Teismann P, et al. Is prostaglandin E(2) a pathogenic factor in amyotrophic lateral sclerosis? Ann Neurol. 2006;59(6):980–3. https://doi.org/10.1002/ana.20847.

72. Lerman BJ, Hoffman EP, Sutherland ML, et al. Deletion of galectin-3 exacerbates microglial activation and accelerates disease progression and demise in a SOD1(G93A) mouse model of amyotrophic lateral sclerosis. Brain Behav. 2012;2(5):563–75. https://doi.org/10.1002/brb3.75.

73. Haidet-Phillips AM, Hester ME, Miranda CJ, et al. Astrocytes from familial and sporadic ALS patients are toxic to motor neurons. Nat Biotechnol. 2011;29(9):824–8. https://doi.org/10.1038/nbt.1957.

74. Swarup V, Phaneuf D, Dupre N, et al. Deregulation of TDP-43 in amyotrophic lateral sclerosis triggers NF-κB-mediated pathogenic pathways. J Exp Med. 2011;208(12):2429–47. https://doi.org/10.1084/jem.20111313.

75. Frakes AE, Ferraiuolo L, Haidet-Phillips AM, et al. Microglia induce motor neuron death via the classical NF-κB pathway in amyotrophic lateral sclerosis. Neuron. 2014;81(5):1009–23. https://doi.org/10.1016/j.neuron.2014.01.013.

76. Alexianu ME, Ho BK, Mohamed AH, et al. The role of calcium-binding proteins in selective motoneuron vulnerability in amyotrophic lateral sclerosis. Ann Neurol. 1994;36(6):846–58. https://doi.org/10.1002/ana.410360608.

77. Marambaud P, Dreses-Werringloer U, Vingtdeux V. Calcium signaling in neurodegeneration. Mol Neurodegener. 2009;4:20. https://doi.org/10.1186/1750-1326-4-20.

78. Heath PR, Shaw PJ. Update on the glutamatergic neurotransmitter system and the role of excitotoxicity in amyotrophic lateral sclerosis. Muscle Nerve. 2002;26(4):438–58. https://doi.org/10.1002/mus.10186.

79. Culmsee C, Semkova I, Krieglstein J. NGF mediates the neuroprotective effect of the β2-adrenoceptor agonist clenbuterol in vitro and in vivo: evidence from an NGF-antisense study. Neurochem Int. 1999;35(1):47–57. https://doi.org/10.1016/s0197-0186(99)00032-7.

80. Gleeson LC, Ryan KJ, Griffin EW, et al. The β2-adrenoceptor agonist clenbuterol elicits neuroprotective, anti-inflammatory and neurotrophic actions in the kainic acid model of excitotoxicity. Brain Behav Immun. 2010;24(8):1354–61. https://doi.org/10.1016/j.bbi.2010.06.015.

81. Ekestern E. Neurotrophic factors and amyotrophic lateral sclerosis. Neurodegener Dis. 2004;1(2–3):88–100. https://doi.org/10.1159/000080049.

82. Kasarskis EJ, Scarlata D, Hill R, et al. A retrospective study of percutaneous endoscopic gastrostomy in ALS patients during the BDNF and CNTF trials. J Neurol Sci. 1999;169(1–2):118–25. https://doi.org/10.1016/s0022-510x(99)00230-0.

83. Miller RG, Petajan JH, Bryan WW, et al. A placebo-controlled trial of recombinant human ciliary neurotrophic (rhCNTF) factor in amyotrophic lateral sclerosis. Ann Neurol. 1996;39(2):256–60. https://doi.org/10.1002/ana.410390215.

84. Lai EC, Felice KJ, Festoff BW, et al. Effect of recombinant human insulin-like growth factor-I on progression of ALS. A placebo-controlled study. The North America ALS/IGF-I Study Group. Neurology. 1997;49:1621–30. https://doi.org/10.1212/WNL.49.6.1621.

85. Borasio GD, Robberecht W, Leigh PN, European ALS/IGF-I Study Group, et al. A placebo-controlled trial of insulin-like growth factor-I in amyotrophic lateral sclerosis. Neurology. 1998;51(2):583–6. https://doi.org/10.1212/wnl.51.2.583.

86. Sorenson EJ, Windbank AJ, Mandrekar JN, et al. Subcutaneous IGF-1 is not beneficial in 2-year ALS trial. Neurology. 2008;71(22):1770–5. https://doi.org/10.1212/01.wnl.0000335970.78664.36.

87. Timmer LT, Hoogaars WMH, Jaspers RT. The role of IGF-1 signaling in skeletal muscle atrophy. Adv Exp Med Biol. 2018;1088:109–37. https://doi.org/10.1007/978-981-13-1435-3_6.

88. McCarthy JJ, Esser KA. Anabolic and catabolic pathways regulating skeletal muscle mass. Curr Opin Clin Nutr Metab Care. 2010;13(3):230–5. https://doi.org/10.1097/MCO.0b013e32833781b5.

89. Adams GR, McCue SA. Localized infusion of IGF-I results in skeletal muscle hypertrophy in rats. J Appl Physiol. 1998;84(5):1716–22. https://doi.org/10.1152/jappl.1998.84.5.1716.

90. Dodge JC, Haidet AM, Yang W, et al. Delivery of AAV-IGF-1 to the CNS extends survival in ALS mice through modification of aberrant glial cell activity. Mol Ther. 2008;16(6):1056–64. https://doi.org/10.1038/mt.2008.60.

91. Palazzolo I, Stack C, Kong L, et al. Overexpression of IGF-1 in muscle attenuates disease in a mouse model of spinal and bulbar muscular atrophy. Neuron. 2009;63(3):316–28. https://doi.org/10.1016/j.neuron.2009.07.019.